Downloaded from orbit.dtu.dk on: Oct 22, 2020

DTU Library

A Correction of Random Incidence Absorption Coefficients for the Angular Distribution of Acoustic Energy under Measurement Conditions

Jeong, Cheol-Ho

Published in:
Journal of the Acoustical Society of America

Link to article, DOI:
10.1121/1.3081392

Publication date:
2009

Document Version
Publisher's PDF, also known as Version of record

Link back to DTU Orbit

Citation (APA):
Jeong, C-H. (2009). A Correction of Random Incidence Absorption Coefficients for the Angular Distribution of Acoustic Energy under Measurement Conditions. *Journal of the Acoustical Society of America*, *125*(4), 2064-2071. https://doi.org/10.1121/1.3081392

General rights
Copyright and moral rights for the publications made accessible in the public portal are retained by the authors and/or other copyright owners and it is a condition of accessing publications that users recognise and abide by the legal requirements associated with these rights.

- Users may download and print one copy of any publication from the public portal for the purpose of private study or research.
- You may not further distribute the material or use it for any profit-making activity or commercial gain
- You may freely distribute the URL identifying the publication in the public portal

If you believe that this document breaches copyright please contact us providing details, and we will remove access to the work immediately and investigate your claim.

A correction of random incidence absorption coefficients for the angular distribution of acoustic energy under measurement conditions

Cheol-Ho Jeong[a)]
Department of Electrical Engineering, Acoustic Technology, Technical University of Denmark (DTU), DK-2800 Kgs. Lyngby, Denmark

(Received 18 June 2008; revised 24 November 2008; accepted 19 January 2009)

Most acoustic measurements are based on an assumption of ideal conditions. One such ideal condition is a diffuse and reverberant field. In practice, a perfectly diffuse sound field cannot be achieved in a reverberation chamber. Uneven incident energy density under measurement conditions can cause discrepancies between the measured value and the theoretical random incidence absorption coefficient. Therefore the angular distribution of the incident acoustic energy onto an absorber sample should be taken into account. The angular distribution of the incident energy density was simulated using the beam tracing method for various room shapes and source positions. The averaged angular distribution is found to be similar to a Gaussian distribution. As a result, an angle-weighted absorption coefficient was proposed by considering the angular energy distribution to improve the agreement between the theoretical absorption coefficient and the reverberation room measurement. The angle-weighted absorption coefficient, together with the size correction, agrees satisfactorily with the measured absorption data by the reverberation chamber method. At high frequencies and for large samples, the averaged weighting corresponds well with the measurement, whereas at low frequencies and for small panels, the relatively flat distribution agrees better.
© *2009 Acoustical Society of America.* [DOI: 10.1121/1.3081392]

PACS number(s): 43.55.Ev, 43.55.Nd [LMW] Pages: 2064–2071

I. INTRODUCTION

A diffuse field is an idealized concept, and it is the basis of several standardized measurements, e.g., the absorption of materials, the sound power of noise sources, and the transmission loss of walls. For a perfectly diffuse field, two assumptions must be satisfied (for example, see Ref. 1).

(1) The local energy density in a room is uniform (the spatial diffusion).
(2) The energy is uniformly incident onto a surface from all directions (the directional diffusion).

In a reverberation room except regions near boundaries, the first condition may be satisfied. At locations about one wavelength apart from boundaries, the deviation of sound pressure is bounded within 1 dB in a large reverberation chamber (0.7λ from corners and edges and 0.25λ from surfaces).[2] Despite attempts to obtain a diffuse sound field in a reverberation room, the second assumption of the random incidence is very hard to fulfill. In particular, when a test specimen covers one surface as in the absorption and sound transmission loss measurement, an ideal diffusivity is rarely obtained. As a compensation, truncation of the angle of incidence was introduced in the calculation of transmission loss, and typical values of the limiting angle vary from 70° to 85° based on empirical data.[3,4] This implies that acoustic energies are not uniformly incident on a sample surface. From this observation, one may deduce that grazingly incident energies are negligible.

The random incidence absorption coefficient is based on the assumption that the intensities of the incident sound are uniformly distributed over all possible directions. In addition, a random distribution of phase of the wave incident on the wall is also assumed. These assumptions result in Paris formula associated with $\sin(2\theta)$.[5] However, the measured absorption coefficient by Sabine's formula (sometimes referred to as the Sabine absorption coefficient) shows a significant discrepancy compared with the random incident coefficient from measured impedance data.[6] It is known that measured absorption coefficients are overestimated for small absorber samples and sometimes exceed unity, even for a nearly locally reacting surface. Theoretically, the random incidence absorption coefficient cannot exceed 0.951 for the specific surface impedance of 1.567. Reasons for the overestimation have been widely accepted to be the finite size of samples and the edge diffraction.[7–12]

To match the theoretical values with measured data, several works have been studied. Concerning the sound transmission loss, de Bruijn[13] addressed the influence of the degree of diffusivity in measurement conditions. Kang *et al.*[14] employed several Gaussian weighting functions for the calculation of sound transmission loss to achieve better agreements with the measurement. Kang *et al.*[15] also measured the incident energy density onto a sample in a reverberation chamber using sound intensimetry. The measured incident intensity decreases with increasing incidence angle; however,

a)Author to whom correspondence should be addressed. Electronic mail: chj@elektro.dtu.dk

 0001-4966/2009/125(4)/2064/8/$25.00 © 2009 Acoustical Society of America

it becomes rather uniform at low frequencies. For the absorption measurement, Makita and Fujiwara[16] investigated possible maximum and minimum values of absorption coefficients assuming non-uniform incident energy, although they had no idea of the angular distribution of the incident energy distribution. They tested unrealistic weighting functions, but this research revealed that the absorption coefficient can exceed unity depending on the directional energy distribution. Makita and Hidaka[17] suggested a revised cosine law of oblique incident energy considering the effective mean free paths of sound rays and reverberation time. However, this modified function is not experimentally validated. Thomasson[18,19] concentrated mainly on the size effect of an absorbing sample, by introducing the concept of averaged radiation impedance. The averaged radiation impedance varies with panel size and aspect ratio under the assumption that the radiation impedance depends weakly on the azimuth angle. However, an ideal diffuse field was assumed in his study. Several semi-empirical corrections have also been suggested. London[20] defined a quantity called the equivalent real impedance and used this quantity for computing the reverberation absorption coefficient. Atal[21] suggested an empirical correction by multiplying a frequency-dependent complex quantity in the form of $(a+bj)$. Dämmig[22] examined the effect of sample locations and room shapes on the sound absorption using the ray tracing method. This work is based on statistical analyses of incidence angles, not the incident energies, to explain the variation of measured absorption coefficients in several source locations and rooms.

In the present study, angular distributions of energy density incident onto an absorbing sample have been investigated using the beam tracing method. The final objective of this study is to improve the agreement by weighting the calculated absorption coefficient according to the actual incident energy density instead of assuming an ideally diffuse incident field.

II. ANGULAR DISTRIBUTION OF ENERGY DENSITY AS A WEIGHTING FUNCTION

First of all, the angular distribution of the reverberant energy density must be calculated. In this study, the beam tracing method[23–25] is employed to simulate the sound propagation in a reverberation chamber. Triangular beams, which are emitted from a source, are followed by their central axes (hereafter rays) without splitting algorithm.[26,27] Instead of splitting beams when beams intersect more than one surface at edges or corners, a large number of beams having a sufficiently small solid angle emanate and illuminate a reverberant field. Only specular reflection is adopted during the tracing, and a negligible absorption coefficient of 0.01 is assigned for all surfaces of a reverberation chamber irrespective of the frequency. The incidence angles and energies coming from these angles, which are computed by the geometrical acoustics technique, will eventually construct an angular distribution of incident energy density as a function of the incidence angle.

Two chambers were chosen as test examples: one is a rectangular parallelepiped chamber and the other is a room

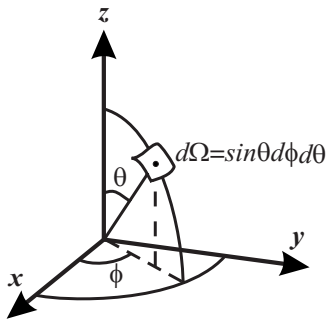

FIG. 1. Spherical polar coordinate representing solid angle element.

with non-parallel surfaces. In accordance with ISO 354 (Ref. 28) and ASTM C 423–02,[29] the sources are located at trihedral corners of the rooms. The assumption that an absorber sample covers one whole surface of the room facilitates the simulation in a way that one can collect all the information of beams incident onto the specific surface. This surface, on which an absorber is installed, is called a target surface.

During the beam tracing, the information on the directional energies and angles of incidence is saved. Acoustic energy decays inversely proportional to r^2 and it is reduced by $(1-\alpha_i)$ whenever beam hits surfaces. Here, r denotes the traveling distance and α_i denotes the absorption coefficient of the ith surface. For a steady-state condition, a total directional energy from θ_i is calculated by summing all components over an interval, $[\theta_{i,l}\ \theta_{i,u}]$. Here, $\theta_{i,l}$ and $\theta_{i,u}$ are the lower and upper limits of the interval, respectively, and θ_i is the arithmetic mean of two limiting values. The directional energy density is the ratio between the total incident sound energy, E_θ, and the corresponding solid angle, Ω_θ. Using a generalized concept of solid angle in terms of spherical polar coordinates, θ and ϕ, respectively (see Fig. 1), the solid angle element is expressed as $d\Omega=\sin\theta d\phi d\theta$. By integrating the azimuth angle, ϕ, from 0 to 2π and the polar angle, θ, over the corresponding interval of $[\theta_{i,l}\ \theta_{i,u}]$, one can find the solid angle at θ_i, as follows:

$$\Omega_{\theta_i}=\int_0^{2\pi}\int_{\theta_{i,l}}^{\theta_{i,u}} d\Omega=\int_0^{2\pi}\int_{\theta_{i,l}}^{\theta_{i,u}} \sin\theta d\theta d\phi$$
$$=2\pi\int_{\theta_{i,l}}^{\theta_{i,u}} \sin\theta d\theta. \quad (1)$$

The solid angle in Eq. (1) increases with the angle of incidence. The directional energy density is defined as the total directional energy incident over the interval of $[\theta_{i,l}\ \theta_{i,u}]$ divided by the corresponding solid angle as follows:

$$D(\theta_i)=\frac{E_{\theta_i}}{\Omega_{\theta_i}}. \quad (2)$$

When the reverberant energy density is computed, the result will be utilized as a weighting function in the calculation of absorption coefficient. In Sec. V, the effect of weighting functions will be discussed by comparing the angle-weighted absorption coefficients with the measured absorption data in a reverberation chamber.

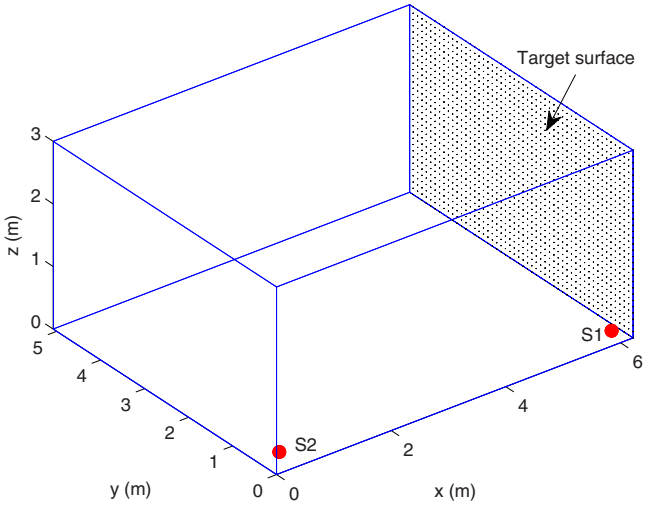

FIG. 2. (Color online) A rectangular room. Target surface is (6.2 m, y, z) plane and two corner sources are located at (6 m, 0.2 m, 0.1 m) and (0.2 m, 0.2 m, 0.2 m), respectively.

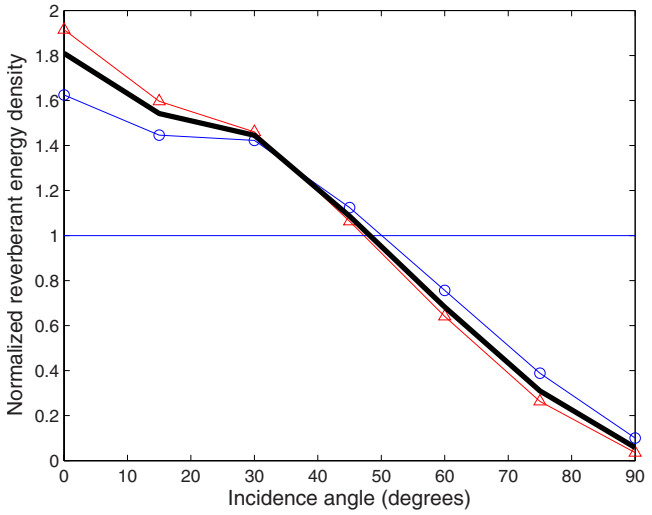

FIG. 3. (Color online) A comparison of reverberant energy density for two corner sources. (—○—) S1 at (6 m, 0.2 m, 0.1 m), (—△—) S2 at (0.2 m, 0.2 m, 0.2 m), and (thick solid line) averaged distribution over 90 source locations.

III. A RECTANGULAR ROOM

In general, lecture rooms and some reverberation chambers are rectangular. This kind of room usually has the problem that the interference is strong due to pairs of parallel surfaces. In this study, all surfaces are assumed smooth, and scattering is not taken into account.

A test rectangular room model is shown in Fig. 2. The edge lengths are 6.2 m, 5.1 m, 3.0 m, and the volume is 94.8 m^3. The target surface of interest is parallel to the y-z plane and located at (6.2 m, y, z). In order to examine the effect of source locations, two possible source locations are chosen in accordance with ISO 354[28] and ASTM C 423–02:[29] According to the standards, a loudspeaker should face into the trihedral corners of a room. The first source, S1, is located at (6 m, 0.2 m, 0.1 m) and S2 is located at (0.2 m, 0.2 m, 0.2 m). In the simulation, 8000 beams were used to scan the space. The number of reflections per beam is limited to 50. It goes without saying that directly transmitted energies from the sources to the target surface contribute the most owing to the shortest distance of propagation. (It is not allowed to place a source near a specimen in measuring the sound transmission loss because the direct radiation is too dominant.)

Incident energy densities for two sources are shown in Fig. 3, which are similar to the energy distributions of direct rays, because the directly transmitted energy overwhelms the total acoustic energy. This normalized energy density shows a similarity with the results by Kang and co-workers.[14,15] Because the source S2 is far from the target surface, only a few direct rays (172 out of 8000) strike the surface. It was found that there is an upper limiting angle of direct incidence, 42° for S2 case. That means there is no directly incident intensity above 42°. Accordingly the normally incident energy is higher than the obliquely incident energy. The acoustic energy density from the normal direction (0°) for S2 is 18% higher than that for S1, due to the lack of obliquely incident direct rays. It can be summarized that when a source is located far from the surface, the normally incident energy is more highlighted, whereas more energies from oblique directions are incident onto the surface for source locations close to the surface.

For 90 equally spaced ($6\times5\times3$) source locations, the average angular distribution of reverberant energy density was simulated and displayed in Fig. 3 (thick line). Sources are distributed by combining x values of (1, 2, 3, 4, 5, 6 m) and y values of (1, 2, 3, 4, 5 m) and z values of (0.2, 1.1, 2 m). The averaged reverberant energy density clearly shows that the acoustic energy density above 80° is lower than 0.2, which will be considered negligible.

IV. A ROOM WITH NON-PARALLEL SURFACES

In Fig. 4, a reverberation room with non-parallel surfaces is shown. The volume of the space is 179 m^3 and the

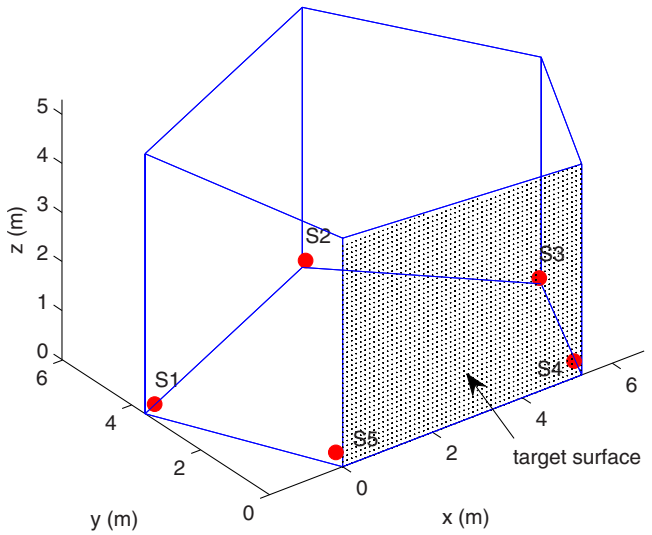

FIG. 4. (Color online) An irregularly shaped room. Target surface is (x, 0, z) plane and five corner sources are located at (−1.5 m, 3.5 m, 0.2 m), (3.7 m, 5.9 m, 0.2 m), (6.6 m, 2.9 m, 0.2 m), (5.3 m, 0.2 m, 0.2 m), and (0 m, 0.2 m, 0.2 m), respectively.

TABLE I. Geometrical nodal data of a reverberation chamber in Fig. 4.

Node numbering	Coordinate		
	x (m)	y (m)	z (m)
1	0	0	0
2	5.32	0	0
3	6.71	2.99	0
4	3.72	6.02	0
5	−1.63	3.61	0
6	0	0	4.66
7	5.32	0	4.30
8	6.71	2.99	4.62
9	3.72	6.02	5.30
10	−1.63	3.61	5.30

absorption coefficient is also 0.01, irrespective of surface and frequency. Geometrical nodal points of the model are listed in Table I. The target surface is x-z plane. Simulations were carried out for five trihedral corner sources shown in Fig. 4.

Figure 5 shows the normalized energy density for five corner sources. For source S1, direct rays from the normal direction cannot reach the target surface. The lowest direct angle of incidence is 23°. By only considering direct sound, the energy density shows a single peak at 45° due to the non-existence of the normal components. However, the reverberant energy density has two peaks at 0° and 45°. This result is apparently different from the rectangular room result, which shows a decreasing tendency with the angle of incidence. The energy is re-distributed due to the lack of direct normal incident rays.

The source S2 is located at the farthest distance of all sources. A high energy density value was found for the normally incident direct ray, as expected. As discussed in Sec. III, a long distance between a source and a target surface emphasizes the importance of the normal direction. An abrupt decrease was found above 45° and the contribution becomes less than 0.5.

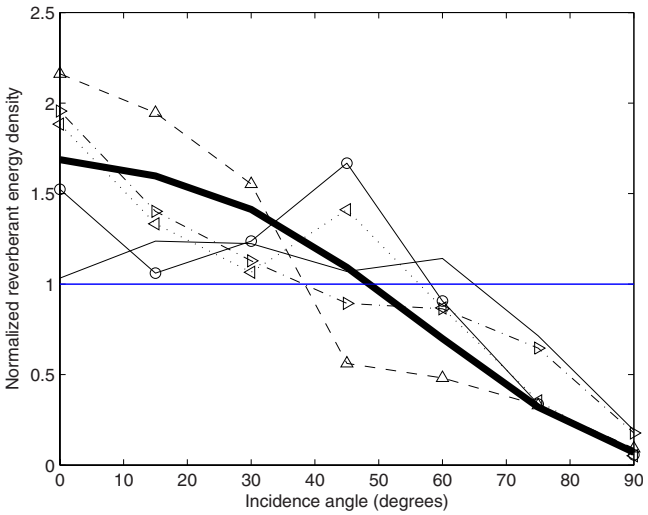

FIG. 5. (Color online) A comparison of angular reverberant energy densities for five corner sources. (—○—) S1, (--△--) S2, (···◁···) S3, (·–▷·–) S4, (—) S5, and (thick solid line) averaged distribution over 96 source locations.

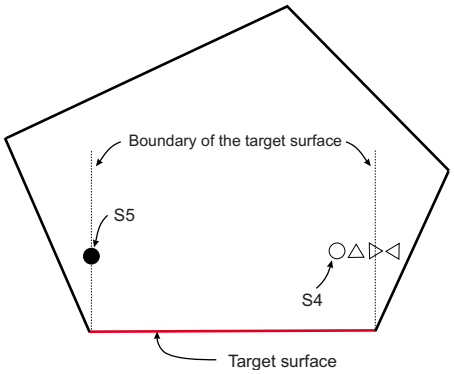

FIG. 6. (Color online) Source locations of S4 and S5 in plane view.

For source S3, the incident energy density shows a strong similarity with that of S1. As the sound source is invisible from the normal direction of the target surface, the incidence angle of 45° becomes pronounced. Therefore a double peak shaped distribution was found for the reverberant acoustic energy density.

The remaining two source locations, S4 and S5, at (5.3 m, 0.2 m, 0.2 m) and (0 m, 0.2 m, 0.2 m), respectively, are situated closer to the target surface. The reverberant acoustic energy densities of two cases show a large difference: The energy continuously decreases for S4, while it is relatively uniform until 60° for S5. In Fig. 6, source locations are illustrated. While the shaded source is located perpendicularly from the boundary of the target surface, two unshaded sources (circle and triangle) are located within the boundary of the target surface. If the source is located within the boundary, the normally incident energy is too pronounced.

Figure 7, which shows the effects of source locations, supports the above statement. By changing x-coordinate of a sound source position from 5.3 to 5.33 m with a step of 0.01 m, one can clearly see that the normal energy density loses its importance, when the source moves away from the surface boundary (refer to the symbols in Fig. 6). When a

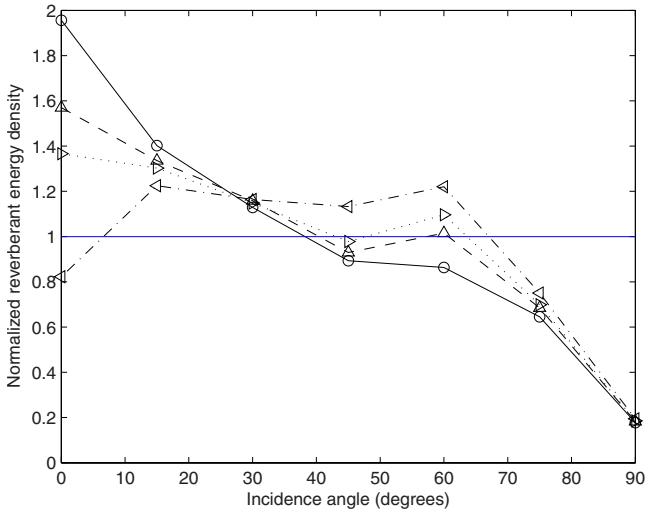

FIG. 7. (Color online) A comparison of reverberant energy densities. x-coordinate of sources varies from 5.30 to 5.33 m with a step of 0.01 m. (—○—) x=5.30 m, (--△--) x=5.31 m, (···▷···) x=5.32 m, and (·–◁·–) x=5.33 m (see Fig. 6).

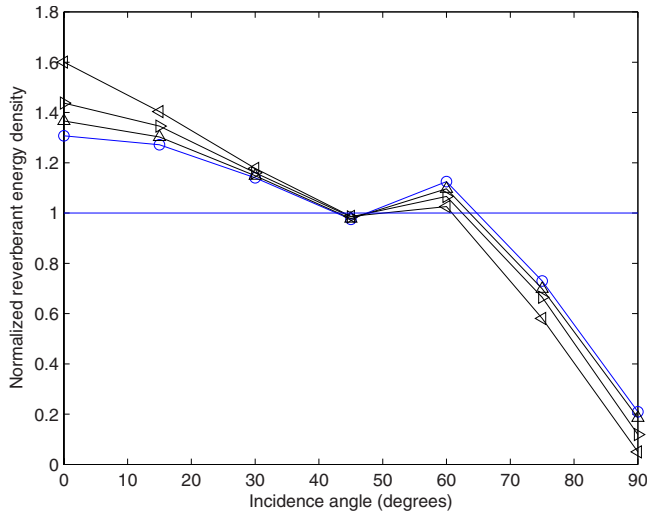

FIG. 8. (Color online) Effects of distance on the reverberant energy densities. (—○—) d=0.01 m, (—△—) d=0.20 m, (—▷—) d=0.50 m, and (—◁—) d=1.00 m. x-coordinate of sources is set to 5.32 m.

source is located outside the boundary, absence of direct normal components decreases overall reverberant energy density for the normal incidence. In order to have a relatively uniform energy distribution, it is desirable to locate the acoustic center of sound source perpendicularly from the surface boundary.

In Fig. 8, effects of a distance between the source and the target surface are shown. Provided that the x-coordinate of source locations is fixed to 5.32 m (perpendicularly from the boundary), distances from the surface to the source were changed to 0.01, 0.2, 0.5, and 1 m. The shorter the distance, the more uniform the reverberant acoustic energy is. It can be concluded that the preferable source location for the uniform reverberant energy is the closest possible and perpendicularly from the boundary of the target surface. For a rectangular room, the ideal position does not exist, because all possible locations are found within the boundary of the target surface.

The thick line in Fig. 5 shows the averaged result over 96 equi-spaced source locations in the irregularly shaped room. The averaged result corresponds well with the rectangular room result, shown in Fig. 3. The calculated reverberant energy densities will be used as a weighting factor in computing absorption coefficients from surface impedances.

V. COMPARISONS WITH THE MEASUREMENT

In Fig. 9, an absorption chart in terms of the real and imaginary parts of the impedance is shown when adopting the averaged energy density for the rectangular room. The solid line and the broken line represent the random incidence absorption coefficient and the angle-weighted absorption coefficient, respectively, calculated as follows:

$$\alpha_{\text{infinite,random}} = \int_0^{\pi/2} \alpha_\theta \sin(2\theta) d\theta, \tag{3a}$$

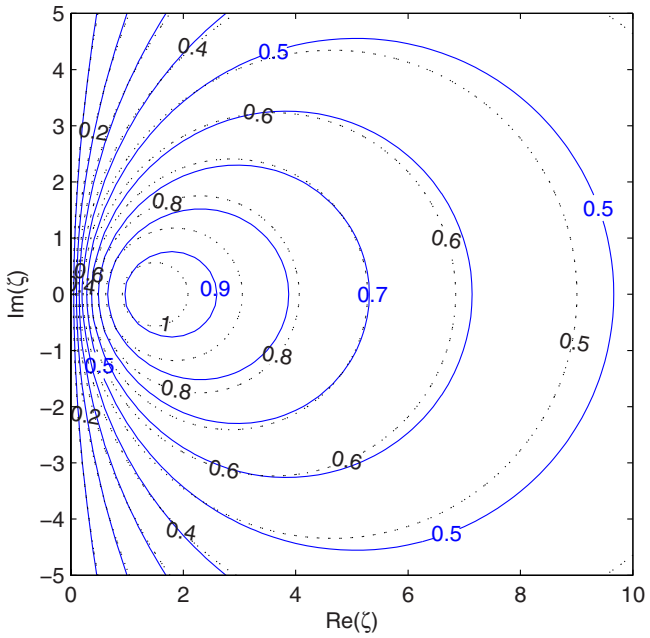

FIG. 9. (Color online) An absorption chart in terms of real and imaginary parts of specific impedance. (——) uniform incidence; (----) angle-weighted.

$$\alpha_{\text{infinite,weighted}} = \int_0^{\pi/2} \alpha_\theta w(\theta) \sin(2\theta) d\theta. \tag{3b}$$

Here, α_θ means the angle dependent absorption coefficient and $w(\theta)$ is the weighting function. According to this chart, if the absorption coefficient is between 0.7 and 0.8, the angle-weighted absorption coefficients are similar to the random incidence absorption coefficients. It is apparent that the maximum random incidence absorption coefficient is less than unity, while the angle-weighted absorption can exceed unity, as in actual reverberation chamber measurements, inside the smallest circle. It should be noted that the result in Fig. 9 cannot be generalized, because the specific weighting function was employed. Moreover, the panel is assumed to be infinitely extended.

It is always necessary to consider the size effect in calculating absorption coefficients. In this study, Thomasson's size correction[18,19] for a finite rectangular panel was adopted. The absorption coefficient for a finite panel is computed using the concept of averaged field impedance as follows:

$$\alpha_{\text{fin}}(\theta) = \frac{4\ \text{Re}(Z_w)}{|Z_w + \bar{Z}_f|^2}. \tag{4}$$

Here, θ is the incidence angle, Z_w is the wall impedance, and $\bar{Z}_f$ is the averaged field impedance over azimuth angle from 0 to 2π expressed as $\bar{Z}_f = 1/2\pi \int_0^{2\pi} Z_f d\phi$. Z_f is the field impedance (sometimes called the radiation impedance) of the wall, which means the impedance of the vibrating surface that radiates sound in the surrounding medium. The field impedance is known as $1/\cos\theta$ for an infinitely large plate; however, the field impedance for a finite sample differs from $1/\cos\theta$, in particular, near grazing incidence.[18,19,30] The field impedance for a finite panel is expressed as follows [see Ref. 18, Eq. (18) and Ref. 19, Eq. (A1)]:

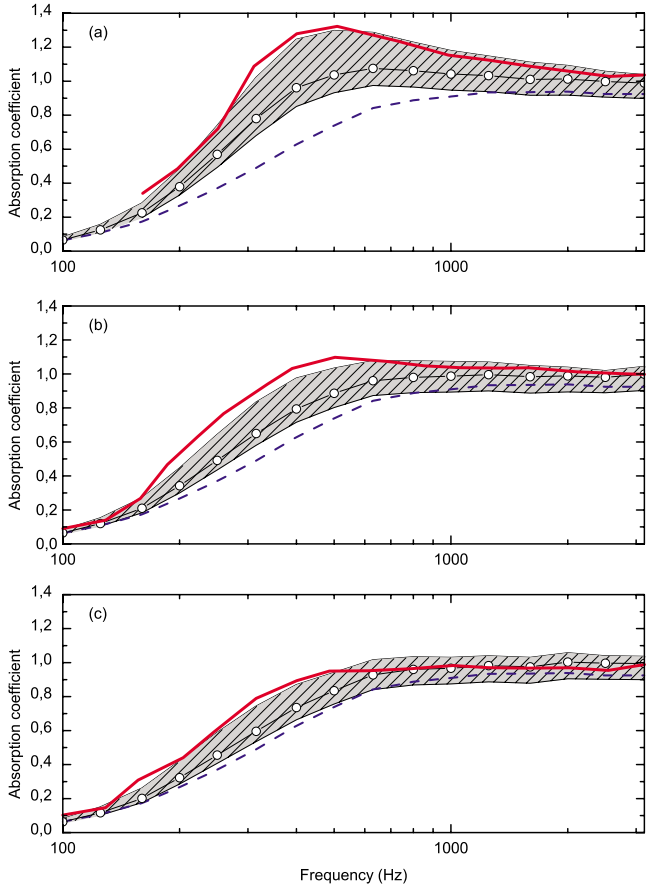

FIG. 10. (Color online) A comparison of absorption coefficient between the reverberation chamber measurement and the angle-weighted value calculated from Z_w. (——) measurement and (—○—) absorption adopting the averaged weighting function. (gray hatched area) Possible range of the angle-weighted absorption coefficient and (– –) random incidence absorption. (a) $e=1.2$ m, (b) $e=2.4$ m, and (c) $e=3.6$ m.

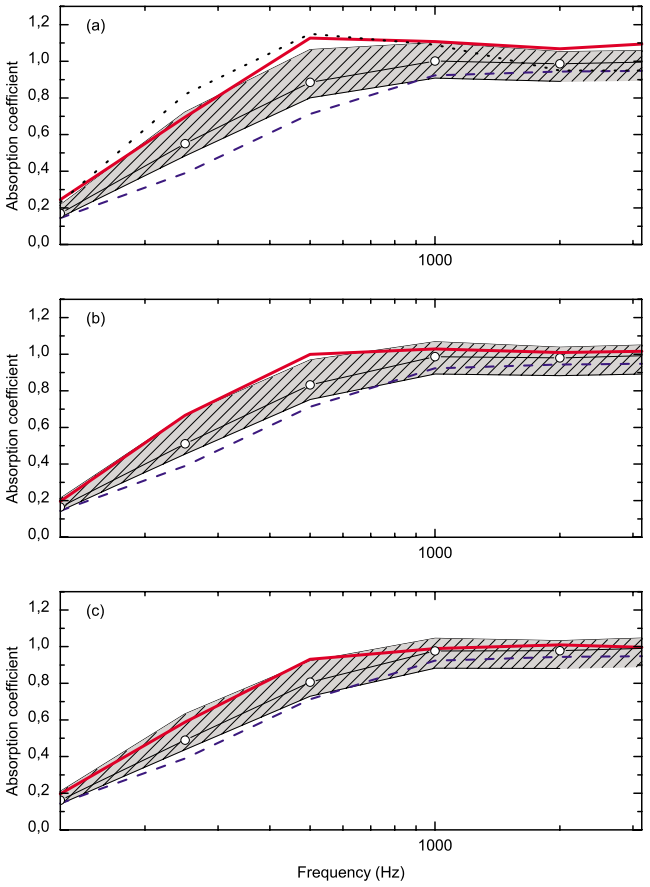

FIG. 11. (Color online) A comparison of absorption coefficient between the reverberation chamber measurement and the angle-weighted value calculated from Z_w. (——) Measurement and (—○—) absorption adopting the averaged weighting function. (gray hatched area) Possible range of the angle-weighted absorption coefficient, (– –) random incidence absorption, and (···) Thomasson's model (Ref. 19). (a) $S=4$ m^2, (b) $S=8$ m^2, and (c) $S=12$ m^2.

$$Z_f = \frac{ik}{S}\int_{S_a}\int\int_{S_a}\int Ge^{ik[\mu_x(x_o-x)+\mu_y(y_o-y)]}dxdydx_ody_o, \quad (5)$$

where k is the wavenumber, $S=\int_{S_a}\int dxdy$, $\mu_x=\sin\theta\cos\phi$, $\mu_y=\sin\theta\sin\phi$, $G=-(2\pi R)^{-1}\exp(ikR)$, and $R=\sqrt{(x-x_o)^2+(y-y_o)^2}$. Consequently the angle-weighted and size-corrected absorption coefficient is calculated as follows:

$$\alpha_{\text{weighted}} = 2\int_0^{\pi/2} w(\theta)\alpha_{\text{fin}}(\theta)\sin(\theta)d\theta$$

$$= 2\int_0^{\pi/2} w(\theta)\frac{4\ \text{Re}(Z_w)}{|Z_w+\bar{Z}_f|^2}\sin(\theta)d\theta, \quad (6)$$

where $w(\theta)$ is the weighting function, which is the angular distribution of energy density by the beam tracing method. The calculated angle-weighted absorption coefficient has been compared with previously published measurements in Figs. 10 and 11. The first absorber consists of 0.05 m thick mineral wool in Thomasson's work.[19] The specific flow resistance and the density of this material were 30 kN s/m^4 and 50 kg/m^3, respectively, and the surface impedance is also taken from Ref. 19. Three kinds of samples were chosen as follows: 1.2×1.2, 2.4×2.4, and 3.6×3.6 m^2. The measured absorption coefficient is the average value from two reverberation chambers with volumes of 190 and 200 m^3, with sufficient diffusion.

The calculated absorption coefficients are shown in Fig. 10 for three different sample sizes. The shaded region denotes a possible range of the angle-weighted absorption coefficient by adopting two limiting angular distributions. The upper curve is obtained by adopting the relatively uniform weighting (for S5 in Fig. 5) and the lower curve is found by adopting the most non-uniform pattern (for S2 in Fig. 5). The hollow circle denotes the angle-weighted absorption coefficient by the averaged weighting function, shown in Fig. 5. Two thick average weighting lines in Figs. 3 and 5 are both similar to a Gaussian distribution. The maximum difference between them is found to be 5% at the normal direction. Because two weighting functions yield nearly the same angle-weighted absorption coefficient, the averaged weighting function in Fig. 5 will be used hereafter. The averaged weighting case can be regarded as a sort of mean value between two limiting absorption coefficients (hereafter, three curves will be named the upper curve, the lower curve, and the averaged weighting, respectively). Large variations in measured data were found depending on sample sizes. In Fig. 10(a), for the smallest sample of edge length (e) of 1.2 m, the maximum value of measured absorption becomes

nearly 1.4. It is apparently due to the size effect, because this kind of overestimation does not occur for the larger two surfaces. One can clearly see that the random incidence absorption from the surface impedance data is far below the measured data. For the smallest sample (a), the measured data correspond well with the upper curve. However, the shaded region becomes narrower, as the frequency increases. When the sample size is four times larger (b), then the measured curve converges to the averaged weighting at high frequencies in Fig. 10(b). Beyond 1 kHz, errors are bounded to 4%. For the largest sample (only this sample is large enough in accordance with ISO 354 specification), the measured curve agrees well with the averaged weighting at frequencies over 800 Hz. One can observe that the measured curve corresponds well with the upper limit value at low frequencies, but the high frequency absorption approaches the averaged weighting case. The three comparisons revealed that the upper curve can be a reasonable guideline at low frequencies.

The second example is the measured data from the second round robin test by Kosten.[11] The material was a rockwool, 5 cm thick, and the density being 100 kg/m^3 (see Ref. 31 for more information, e.g., surface impedance data). Three different surface areas of 4, 8, and 12 m^2 were tested. It should be noted that the measured data are the averaged value over 19 different reverberation chambers all over the world. The degree of diffusion is different from laboratory to laboratory. Dimensions and aspect ratios of samples are not provided. Only the information on sample sizes is given. Samples had different aspect ratios and sometimes different sizes. For example, the surface area varies from 7.5 to 8.25 m^2 for the 8 m^2 sample. Because the author does not have any detailed information on samples, they are regarded as square samples, the edge length e being calculated as $\sqrt{S}$.

Figure 11 shows a comparison between the reverberation chamber measurement and the theoretical angle-weighted absorption coefficient. For the smallest sample in Fig. 11(a), the measured data correspond well with the upper curve, similarly with Fig. 10(a). In this case, Thomasson's model was also compared with the measured data. Thomasson's model[19] seems to agree acceptably below 1 kHz, but it starts to underestimate beyond 1 kHz. In his paper, Thomasson admitted that the deviation at highest frequencies could not be explained. On the other hand, when the proper weighting function is incorporated, the result is improved. It is also observed that the upper curve shows a reasonable guideline at low frequencies and for small size, whereas the averaged weighting agrees well with the measurement for high frequencies and larger samples.

Therefore, a non-dimensionalized parameter, ke, which is multiplication of the wavenumber and the characteristic length of a sample, is introduced to effectively indicate the general trend of the relative errors. A high value of ke means a high frequency and/or a large sample. For small ke, one can see that the upper curves agree well with the measurement. As ke increases, the averaged weighting curve becomes closer to the measurement. The lower curves seem meaningless for all cases, because most of measured absorptions are higher than the angle-weighted absorption coefficient by the averaged weighting function.

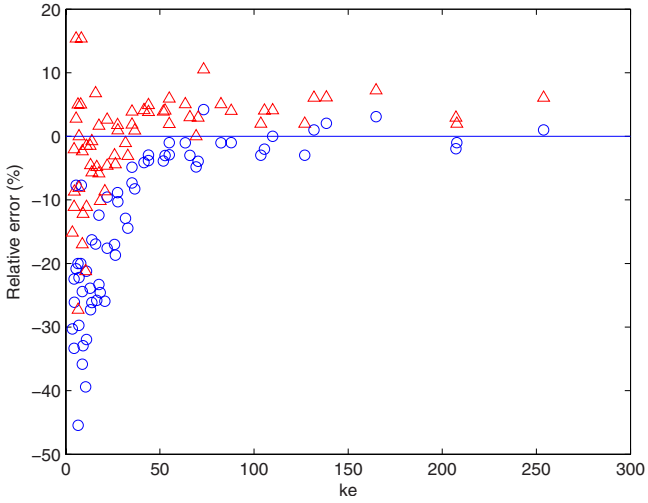

FIG. 12. (Color online) A relative error of the weighted absorption coefficient as a function of ke. (○) Averaged weighting and (△) upper curve.

The relative error of the angle-weighted absorption coefficient is illustrated in Fig. 12. The measured value is used as a reference in defining the relative error. One can see the clear tendency that the error of the averaged weighting function (hollow circle) decreases with increasing ke. The error of upper curve is smaller for low ke, but the error converges to 7% biased from the measurement, as ke becomes higher. One can also observe that the error of the averaged weighting seldom is positive (except five cases), which means the measured value is generally higher than the angle-weighted absorption by the averaged weighting. If ke is higher than 50, the results by the averaged weighting will be acceptable. The upper curve shows smaller errors for low ke, but the error is still too large to be acceptable (the maximum error is 23%). Larger errors at low ke may originate from neglecting diffraction phenomenon in the calculation. It should be mentioned here that the distribution of measured intensity at lower frequency in a reverberant condition is flatter than the intensity distribution at high frequencies in Ref. 15. This fact also supports the better agreement employing the more uniform energy distribution at low frequencies.

It can be summarized that non-uniform energy density can reduce discrepancies between the measured absorption coefficient and the theoretical value when it is taken into account with the size correction. A high value of ke guarantees an acceptable precision by using the averaged weighting, which is similar to a Gaussian distribution.

VI. CONCLUSIONS

The angular distribution of energy density incident on a sample has been simulated for a rectangular room and a reverberation chamber with non-parallel surfaces by using the beam tracing method. A large variation in incident energy density was found depending on the source position. To achieve a uniform distribution, the source should be located perpendicularly from the boundary of the target surface, as close as possible to the target surface. Therefore a room with non-parallel walls is advantageous for obtaining a uniform distribution. A long distance from a source to a target surface

results in a concentration of acoustic energy near the normal direction. The simulated reverberant energy distribution plays the role of a weighting factor in calculating the angle-weighted absorption coefficient. The importance of non-uniform incident energy becomes significant for high ke values. For smaller values of ke, the calculated absorption coefficient adopting fairly uniform distribution agrees well with the measurement, while the averaged Gaussian-like weighting function agrees better with the measurement for high ke.

ACKNOWLEDGMENTS

The author gratefully acknowledges the valuable comments and encouragement from Professor Finn Jacobsen at DTU. The author also would like to thank Dr. Jens Holger Rindel, Dr. Sven-Ingvar Thomasson, Dr. Hyun-Ju Kang, and Professor Jeong-Guon Ih for constructive discussion.

[1]T. J. Schultz, "Diffusion in reverberation rooms," J. Sound Vib. **16**, 17–28 (1971).
[2]R. V. Waterhouse, "Interference patterns in reverberant sound fields," J. Acoust. Soc. Am. **27**, 247–258 (1955).
[3]L. L. Beranek, *Noise Reduction* (McGraw-Hill, New York, 1971).
[4]R. E. Jones, "Inter-comparisons of laboratory determinations of airborne sound transmission loss," J. Acoust. Soc. Am. **66**, 148–164 (1979).
[5]E. T. Paris, "On the reflection of sound from a porous surface," Proc. R. Soc. London, Ser. A **115**, 407–419 (1927).
[6]D. Olynyk and T. D. Northwood, "Comparison of reverberation room and impedance tube absorption measurement," J. Acoust. Soc. Am. **36**, 2171–2174 (1964).
[7]A. de Bruijn, "Influence of diffusivity on the transmission loss of a single-leaf wall," J. Acoust. Soc. Am. **47**, 667–675 (1970).
[8]T. T. Wolde, "Measurements on the edge-effect in reverberation rooms," Acustica **18**, 207–212 (1967).
[9]W. Kuhl, "Der einfluss der kanten auf die schall-absorption poroser materialien (The influence of the edges on sound absorption of the porous materials)," Acustica **10**, 264 (1960).
[10]T. W. Bartel, "Effect of absorber geometry on apparent absorption coefficients as measured in a reverberation chamber," J. Acoust. Soc. Am. **69**, 1065–1074 (1981).
[11]C. W. Kosten, "International comparison measurement in the reverberation room," Acustica **10**, 400–411 (1960).
[12]P. E. Sabine, "Specific normal impedances and sound absorption coefficients of material," J. Acoust. Soc. Am. **12**, 317–322 (1941).
[13]A. de Bruijn, "Influence of diffusivity on the transmission loss of a single leaf wall," J. Acoust. Soc. Am. **47**, 667–675 (1970).
[14]H.-J. Kang, J.-G. Ih, J.-S. Kim, and H.-S. Kim, "Prediction of sound transmission loss through multilayered panels by using Gaussian distribution of directional incident energy," J. Acoust. Soc. Am. **107**, 1413–1420 (2000).
[15]H.-J. Kang, J.-G. Ih, J.-S. Kim, and H.-S. Kim, "An experimental investigation on the directional distribution of incident energy for the prediction of sound transmission loss," Appl. Acoust. **63**, 283–294 (2002).
[16]Y. Makita and K. Fujiwara, "Effects of precision of a reverberant absorption coefficient of a plane absorber due to anisotropy of sound energy flow in a reverberation room," Acustica **39**, 331–335 (1978).
[17]Y. Makita and T. Hidaka, "Revision of the cos theta law of oblique incident sound energy and modification of the fundamental formulations in geometrical acoustics in accordance with the revised law," Acustica **63**, 163–173 (1987).
[18]S.-I. Thomasson, "On the absorption coefficient," Acustica **44**, 265–273 (1980).
[19]S.-I. Thomasson, "Theory and experiments on the sound absorption as function of the area," Report No. TRITA-TAK 8201, KTH, Stockholm, Sweden, 1982.
[20]A. London, "The determination of reverberant sound absorption coefficients from acoustic impedance measurements," J. Acoust. Soc. Am. **22**, 263–269 (1950).
[21]B. S. Atal, "A semi-empirical method of calculating reverberation chamber coefficients from acoustic impedance value," Acustica **9**, 27–30 (1959).
[22]P. Dämmig, "Model investigation into sound fields in reverberation rooms," Acustica **75**, 105–120 (1991).
[23]T. Lewers, "A combined beam tracing and radiant exchange computer-model of room acoustics," Appl. Acoust. **38**, 161–178 (1993).
[24]A. Wareing and M. Hodgson, "Beam-tracing model for predicting sound field in rooms with multilayer bounding surfaces," J. Acoust. Soc. Am. **118**, 2321–2331 (2005).
[25]C.-H. Jeong, J.-G. Ih, and J. H. Rindel, "An approximate treatment of reflection coefficient in the phased beam tracing method for the simulation of enclosed sound fields at medium frequencies," Appl. Acoust. **69**, 601–613 (2008).
[26]I. A. Drumm and Y. W. Lam, "The adaptive beam-tracing algorithm," J. Acoust. Soc. Am. **107**, 1405–1412 (2000).
[27]T. Funkhouser, N. Tsingos, I. Carlbom, G. Elko, M. Sondhi, J. E. West, G. Pingali, P. Min, and A. Ngan, "A beam tracing method for interactive architectural acoustics," J. Acoust. Soc. Am. **115**, 739–756 (2004).
[28]ISO, "Acoustics-measurement of sound absorption in a reverberation room," ISO 354 (International organization for Standardization, Geneva, 1985).
[29]"ASME C 423–02: Standard test method for sound absorption and sound absorption coefficients by the reverberation room" (American Society of Mechanical Engineers, New York, 2003).
[30]J. H. Rindel, "Modeling the angle-dependent pressure reflection factor," Appl. Acoust. **38**, 223–234 (1993).
[31]C. W. Kosten, "Die messung der schallabsorption von materialien" (The measurement of sound absorption of the materials)," in Proceedings of the Third International Congress on Acoustics, Stuttgart, Germany (1959), pp. 815–830.